Metallodielectric Colloidal Core−Shell Particles for Photonic Applications

Christina Graf*,† and Alfons van Blaaderen†,‡

Soft Condensed Matter, Debye Institute, Utrecht University, Ornstein Laboratory, Princetonplein 5, 3584 CC Utrecht, The Netherlands, and FOM Institute for Atomic and Molecular Physics, Kruislaan 407, 1098 SJ Amsterdam, The Netherlands

Received July 16, 2001. In Final Form: October 10, 2001

A new approach for the synthesis of colloidal gold shell particles with a dielectric core is described. Small gold nanoclusters were attached to the functionalized surface of colloidal silica particles. Reductive growth and coalescence of these clusters lead to the formation of a closed gold layer. By variation of the thickness of this gold layer and the radius of the shell it is possible to adjust the plasmon resonance of the gold shell particles over the whole visible and infrared region of the spectrum. The optical properties of the particles made are in good agreement with theoretical calculations for core−shell particles. Because of their low polydispersity, these gold shell particles form large crystals with submicron lattice constants. It is also possible to produce hollow gold shells by dissolution of the silica core. Further, a new method to coat the silica core gold shell particles with an additional outer silica shell is presented. This allows for a reduction in the van der Waals forces and facilitates functionalization of the particles for use in various photonic applications.

Introduction

Small (< 200 nm) solid metallic nanoparticles are well-known for their attractive optical properties: a strong optical resonance and a large and fast nonlinear optical polarizability associated with a plasmon frequency of the conduction electrons in the particle.[1−3] In addition, the plasmon resonance can lead to large enhancements in the local electric fields close to the metal surface. These optical properties are explained well by classical electromagnetic theory (Mie theory[4]) and have led to a range of applications, like optical filters,[5] labeling in (electron) microscopy,[6,7] single-electron transistors,[8] and Raman spectroscopy enhancers.[9] In this last example, the enormous enhancement factors of 10^{15} per aggregate of silver particles reported[9] are not yet completely understood. However, the tunability of the resonance of pure metal particles is relatively limited. For instance, the 520 nm resonance of gold particles with a size of 5 nm in water shifts only 25 nm to larger wavelength with an increase in size to 80 nm. Moreover, the synthesis of monodisperse larger (>100 nm) metal particles is still quite hard.[10,11] Shifts due to a change in refractive index of the surrounding medium are modest as well.[12,13] Colloidal metal shells on the other hand can have resonances that can be tuned over a wide range as a function of the core-to-shell ratio. The greatly enhanced ability to manipulate the boundary conditions of the resonating conduction electrons makes it possible to cover theoretically the ultraviolet, visible, and infrared parts of the spectrum.[13] The group of Halas has shown in several papers how such shells composed of gold can be grown around silica colloids and how the single-particle properties can be exploited.[14−17] Silica colloids provide for a convenient dielectric core, as they can be grown with a small polydispersity (<1%),[18] and in addition, methods have been developed to chemically incorporate dyes inside the silica with nanometer precision of the radial position.[19,20]

We are motivated not only by the single-particle properties but also by the prospect of using the collective response of metallodielectric colloids if they are arranged on a regular three-dimensional (3D) lattice. For instance, it has been shown recently that regular 3D structures with feature sizes on the order of the wavelength under consideration, also called photonic crystals, can have a full photonic band gap in the visible, if they are made from metallodielectric spheres.[21−23] The terminology used

* To whom correspondence should be addressed. E-mail: c.graf@phys.uu.nl.
† Utrecht University.
‡ FOM Institute for Atomic and Molecular Physics. E-mail: a.vanblaaderen@phys.uu.nl.

(1) Hache, F.; Richard, D.; Flytzanis, C.; Kreibig, U. *Appl. Phys.* **1988**, *47*, 347.
(2) Bigot, J. Y.; Merle, J. C.; Cregut, O.; Daunois, A. *Phys. Rev. Lett.* **1995**, *75*, 4702.
(3) Perner, M.; Bost, P.; Lemmer, U.; von Plessem, G.; Feldmann, J.; Becker, U.; Menig, M.; Schmitt, M.; Schmidt, H. *Phys. Rev. Lett.* **1997**, *78*, 2192.
(4) Mie, G. *Ann. Phys.* **1908**, *25*, 377.
(5) Dirix, Y.; Bastiaansen, C.; Caseri, W.; Smith, P. C. *Adv. Mater.* **1999**, *11*, 223.
(6) Bendayan, M. *Biotech. Histochem.* **2000**, *75*, 203.
(7) Möller, R.; Csáki, A.; Köhler, J. M.; Fritzsche, W. *Nucleic Acids Res.* **2000**, *28*, e91.
(8) Sato, T.; Hasko, D. G.; Ahmed, H. *J. Vac. Sci. Technol., B* **1997**, *15*, 45.
(9) Nie, S. R.; Emroy, S. R. *Science* **1997**, *275*, 1102.
(10) Brown, K. R.; Walter, D. G.; Natan, M. J. *Chem. Mater.* **2000**, *12*, 306.
(11) Goia, D. V.; Matijevic, E. *Colloid Surf., A* **1999**, *146*, 139.
(12) Liz-Marzan, L. M.; Giersig, M.; Mulvaney, P. *Langmuir* **1996**, *12*, 4329.
(13) Neeves, A. E.; Birnboim, M. H. *J. Opt. Soc. Am.* **1989**, *6*, 787.
(14) Oldenburg, S. J.; Averitt, R. D.; Westcott, S. L.; Halas, N. J. *Chem. Phys. Lett.* **1998**, *288*, 243.
(15) Oldenburg, S. J.; Hale, G. D.; Jackson, J. B.; Halas, N. J. *Appl. Phys. Lett.* **1999**, *75*, 1063.
(16) Oldenburg, S. J.; Jackson, J. B.; Westcott, S. L.; Halas, N. J. *Appl. Phys. Lett.* **1999**, *75*, 2897.
(17) Oldenburg, S. J.; Westcott, S. L.; Averitt, R. D.; Halas, N. J. *Chem. Phys.* **1999**, *111*, 4729.
(18) van Blaaderen, A.; Velikov, K. P.; Hoogenboom, J. P.; Vossen, D. L. J.; Yethiraj, A.; Dullens, R.; van Dillen, T.; Polman, A. Manipulation of colloidal crystallization for photonic applications: from self-organization to do-it-youself-organization. In *Photonic Crystals and Light Localization in the 21st Century*; Soukoulis, C. M., Ed.; Kluwer Academic Publishers: Dordrecht, Boston, London, 2001; Vol. 563, p 239.
(19) van Blaaderen, A.; Vrij, A. *J. Colloid Interface Sci.* **1993**, *156*, 1.
(20) Verhaegh, N. A. M.; van Blaaderen, A. *Langmuir* **1994**, *10*, 1427.

10.1021/la011093g CCC: $22.00
Published on Web 12/18/2001

to describe the optical properties resembles that of solid-state physics, as there is a strong analogy between the propagation of photons in a photonic crystal with a complete band gap and the flow of electrons in a semiconductor. Photonic crystals with a complete or almost complete band gap have the ability to manipulate both the propagation and the spontaneous emission of photons in new and exciting ways, leading to applications such as thresholdless lasers, low loss waveguides with small radii of curvature, splitters, and so forth.[24] Photonic crystals with a complete band gap in the visible have not yet been realized because of the difficulty of achieving submicron structures with a sufficiently high index of refraction contrast. The manipulation of colloidal self-organization or crystallization is a powerful route to create photonic crystals.[18] However, even in applications where the refractive index contrast is relatively modest, like latex spheres in water, interesting photonic properties can be realized with colloidal crystals. For instance, Pan et al.[25] realized an ns optical switch using the refractive index change induced by the absorption of an organic dye and the subsequent heating of the colloids after an intense laser pulse. We expect that the use of metallodielectric spheres, which are much less susceptible to light-induced damage, can significantly improve the properties of this interesting application. Even in the case of 1D and 2D arrangements of small metal spheres, interesting photonic applications relying on nonradiative coupling of plasma resonances have been proposed.[26]

In this paper a modification of the procedure described in refs 14 and 17 to make silica−gold core−shell particles is presented, because it turned out to be impossible to crystallize spheres made according to refs 14 and 17 because of the large amount of irregular solid gold particles that were also formed and could not be removed. Results on crystallization of the monodisperse silica−gold shells will be presented. However, the large van der Waals forces of our gold shell between the particles prevent crystallization at high volume fractions. The necessary increased levels of ionic strength would lead to aggregation instead of crystallization. Therefore, we developed a procedure to grow a smooth silica shell around the gold shell. Not only does this shell reduce the van der Waals interactions significantly, the large knowledge base available for the manipulation of interactions by surface modification that is known for silica becomes available. For silica spheres, several procedures exist to grow close-packed colloidal crystals.[18] In addition, the silica layer allows for controlled placement of dyes close to the metal surface or can be used to induce further growth of silica layers of variable thickness covering the whole colloidal range.[27−29]

In the present paper we will also show how the silica core can be removed from core−shell particles for which the gold shell is almost complete. This procedure works even if extinction data indicate that the shell is practically complete. Empty shells can be filled, for example, with dyes or catalysts and therefore increase the possible use of these particles.

After a description of the experimental synthesis and characterization methods, the morphological properties of the particles as studied by extinction measurements, confocal microscopy, and electron microscopy are discussed and compared to calculations based on the Mie theory of core−shell particles.[30,31] We will end with the first results on crystallization of the metallodielectric spheres.

Experimental Section

(i) Materials. Tetraethoxysilane (TES, ≥98.0%), 3-aminopropyltrimethoxysilane (APS, ≥97%), and sodium silicate solution ($Na_2O(SiO_2)_{3-5}$, 27 wt % SiO_2) were obtained from Fluka. Ethanol (p. a.), ammonia (29.3 wt % NH_3), NaOH (98.5%), K_2CO_3 (99+%), and hydrofluoric acid (38−40%) were purchased from Merck, tetrakishydroxymethylphosphonium chloride (80% aqueous solution) and hydroxylamine hydrochloride (99%) were purchased from Aldrich, and hydrogen tetrachloroaurate(III) hydrate (p. a.) was purchased from Acros Organics. All chemicals were used as received. Water used in the described reactions and cleaning of the glassware was obtained from a PUR1TE Select system from Purite Ltd. and had a measured resistivity of 16 MΩcm.

(ii) Syntheses. The silica-filled, hollow, and silica-covered gold shells were synthesized in a multistep reaction. An outline of the synthesis is shown in Figure 1.

The reaction vessels utilized in all reaction steps with gold or gold salts were cleaned before use with aqua regia to dissolve gold, followed by hydrofluoric acid (8 vol %) to remove insoluble deposits on the glass surface. After that they were copiously rinsed with water. For the synthesis of the silica cores and the coupling of APS to these cores, the reaction vessels were also cleaned with hydrofluoric acid (8 vol %) and after that several times with water. The reaction steps with gold or gold salts were carried out under nitrogen and exclusion of light.

In the following section we will describe representative examples quantitatively. All particle radii and shell thicknesses mentioned in this Experimental Section were measured by transmission electron microscopy (TEM). In calculating concentrations and surface areas from measured weight fractions, we assumed addititivity of volumes, the bulk density of gold (18.9 g/cm^3), and a density of silica of 2.0 g/cm^3.[19]

(a) Gold Shells with a Silica Core. *Gold-Functionalized Silica Particles.* In the first reaction step silica spheres covered with gold particles were prepared using a modification of the method described by Oldenburg et al.[14] and Westcott et al.[32] Silica spheres with a low polydispersity were obtained by first preparing small silica seed particles of $r = 35$ nm radius using the Stöber procedure:[33] 35.41 g of TES and 43 mL of ammonia were added to 1000 mL of ethanol (final concentrations, 0.17 M TES, 0.69 M NH_3, 1.56 M H_2O). In the subsequent reaction steps these particles were grown larger by seeded growth:[27−29] In every step the dispersions were diluted to silica volume fractions of 0.5% and the ammonia and water concentrations were kept at 0.69 M NH_3 and 1.56 M H_2O. TES (30 mL, 0.134 M) was added per 1000 mL of dispersion for each step. Seven and eleven seeded growth steps, respectively, were needed to reach final particle radii of 99 and 205 nm. These silica particles were functionalized with APS by the method described in ref 19. The amount of APS was calculated to be sufficient to provide an approximately 2.5 monolayer coating on the silica particles.[32] The area on the nanoparticle surface covered by each organosilane molecule was assumed to be nominally 0.6 nm^2.[34] For example, 23.6 μL of APS (1.34×10^{-4} M) was added to 200 mL of an ethanolic silica sphere

(21) Moroz, A. *Europhys. Lett.* **2000**, *50*, 466.
(22) Moroz, A. *Phys. Rev. Lett.* **1999**, *83*, 5274.
(23) Zhang, W. Y.; Lei, X. Y.; Wang, Z. L.; Zheng, D. G.; Tam, W. Y.; Chan, C. T.; Sheng, P. *Phys. Rev. Lett.* **2000**, *84*, 2853.
(24) *Photonic Crystals and Light Localization in the 21st Century*; Kluwer Academic Publishers: Dordrecht, Boston, London, 2001; Vol. 563.
(25) Pan, G.; Kesavamoorthy, R.; Asher, S. A. *Phys. Rev. Lett.* **1997**, *78*, 3860.
(26) Brongersma, M. L.; Hartman, J. W.; Atwater, H. A. *Phys. Rev. B* **2000**, *62*, R16356.
(27) Philipse, A. P. *Colloid Polym. Sci.* **1988**, *266*, 1174.
(28) Bogush, G. H.; Zukoski, C. F. *J. Colloid Interface Sci.* **1991**, *142*, 19.
(29) van Blaaderen, A.; van Geest, J.; Vrij, A. *J. Colloid Interface Sci.* **1992**, *154*, 481.
(30) Aden, A. L.; Kerker, M. *J. Appl. Phys.* **1951**, *22*, 1242.
(31) Bohren, C. F.; Huffman, D. R. *Absorption and Scattering of Light by Small Particles*; Wiley: New York, 1984.
(32) Westcott, S. L.; Oldenburg, S. J.; Lee, T. R.; Halas, N. J. *Langmuir* **1998**, *14*, 5396.
(33) Stöber, W.; Fink, A.; Bohn, E. *J. Colloid Interface Sci.* **1968**, *26*, 62.
(34) Waddell, T.; Leyden, D.; DeBello, M. *J. Am. Chem. Soc.* **1981**, *103*, 5303.

Table 1. Growth of the Gold Shells

sample	core radius[a] (nm)	shell thickness[b] (nm)	precursor particles[c] conc (g/L)	precursor particles[c] volume (mL)	$HAuCl_4/K_2CO_3$ volume (mL)	$NH_2OH{\cdot}HCl$ volume (mL)
C1S1	99	33	1	1.55	148	74
C2S1	205	34	7	1.53	700	350
C2S2	205	46	7	1.53	1000	500
C2S3	205	65	2	1.55	442	221
C2S4	205*/244**	88	10	0.54	100	50

[a] Core radius: particle radius obtained by TEM measurements; for sample C2S4, radius of initial silica core (*) and radius of precursor particles (**). [b] Shell thickness: intended shell thickness; used to calculate the volumes of the $HAuCl_4/K_2CO_3$ and $NH_2OH{\cdot}HCl$ solutions. [c] Precursor particles: silica particles covered with small gold clusters (sample C1S1 − C2S3) or silica particles ($r = 205$ nm) with a 39 nm gold shell (C2S4) (see text).

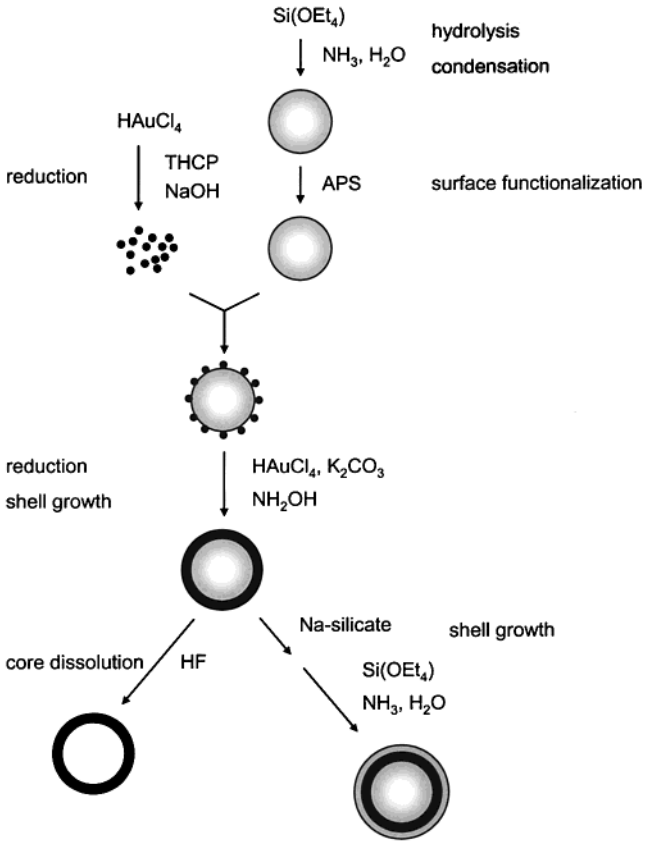

Figure 1. Diagram of the synthesis of gold shells with a silica core, hollow gold shells, and silica-covered gold shells. In the first step, small gold nanoclusters are attached to silica spheres. Reduction of hydrogen tetrachloroaurate on these functionalized spheres leads to the formation of gold shells. By subsequent treatment with hydrofluoric acid, hollow gold shells can be obtained. By consecutive addition of sodium silicate and tetraexthoxysilane, it is possible to cover the gold shell particles with a silica shell.

solution ($r = 205$ nm, $c = 13.8$ g/L). This mixture was stirred for 12 h and then refluxed for 1 h. Excess reactants were removed from the APS-functionalized particles by centrifugation (300 g) and redispersing in pure ethanol at least five times. Silica particles (205 nm radius) with a five times higher initial concentration of APS were made and cleaned in the same way.

Silica particles ($r = 188$ nm) with a fluorescent core ($r = 92$ nm) labeled with the dye rhodamine isothiocyanate (RITC) were also coated with a gold shell. The synthesis and characterization of these particles is described in ref 20. These particles were functionalized in the same way with APS as described above.

Aqueous solutions of small gold nanoclusters (1−2 nm in diameter) were prepared by reduction of chloroauric acid with tetrakishydroxymethylphosphonium chloride (THPC) as described by Duff et al.[35] The concentrations of these gold nanocluster solutions were calculated assuming that all chloroauric acid was reduced to 1.5 nm diameter gold clusters. A freshly prepared gold nanocluster solution (50 mL, $c \approx 9.9 \times 10^{-6}$ mol/L) was diluted with 150 mL of water. Then the amount of silica colloids required to provide a surface area of silica equal to 2.5 times the total cross-sectional area of the small gold nanoclusters was estimated. The corresponding volume of silica spheres solution (e.g., 185 mg of APS-functionalized silica spheres of 205 nm radius in 21.7 mL of ethanol) was diluted with ethanol to 50 mL and added dropwise to the aqueous gold nanocluster solution within 5 min under magnetic stirring (600 rpm). Next, the solution was stirred for another 12 h.

To remove nonattached small gold nanoclusters, the solution was centrifuged (200*g*), the supernatant was removed, and the remaining light brown pellet was redispersed in water. To prevent the growth of pure gold particles during the formation of the gold shell, this centrifugation/redispersion step was repeated until the supernatant practically contained no small gold nanoclusters anymore. This was checked accurately by taking an extinction spectrum of the respective supernatant. (For the spectrum of such small gold nanoclusters, see ref 36.) Finally, the precursor particles were redispersed in 100 mL of water and allowed to age in the refrigerator for about 1 week.

Shell Growth. For this reaction step a method modified from those of Weiser[37] and Duff et al.[38] for the seeded growth of small gold particles was employed. An aliquot (17.4 mL) of a 25 mM chloroauric acid stock solution was diluted with 982.6 mL of water; then 249 mg (1.8 mM) of potassium carbonate was added and the resulting solution was aged at least 1 day in the dark, during which it changed color from yellow to white due to the formation of gold hydroxide.[37,38]

To initiate growth of the gold shell, the precursor silica particles covered with the small gold clusters were added to the aged $HAuCl_4/K_2CO_3$ solution. The ratio of the amount of the precursor particles added to the volume of the gold salt solution depended on the intended thickness of the gold shells. It was calculated assuming all added $HAuCl_4$ would reduce to gold shells around the silica. The radii of the precursor particles and the concentration of the precursor particles solution are given in Table 1.

To this mixture, stirred with a magnetic bar (600 rpm), a freshly prepared hydroxylamine hydrochloride solution (130 mg/L; 1.87 mM; for amounts see Table 1) was added dropwise with a dropping funnel in 45 min. In the case of the particles with the bigger core (205 nm radius), the color of the suspension changed during the addition of the reducing agent from (nearly) colorless over violet and blue to a strongly scattering brown solution. For the smaller cores (99 nm radius) the final suspension showed red scattering and green absorption.

To concentrate the colloidal gold shells for further characterization and to remove excess reagents, these suspensions were centrifuged (50*g*).

To demonstrate that it is possible to growth particles with a thick gold shell (82 nm) by seeded growth, silica particles with a thinner gold shell (39 nm; core radius 205 nm) were used as precursors instead of particles covered with small gold clusters (see sample C2S4 in Table 1). The reaction was carried out as described in the previous paragraphs.

(35) Duff, D. G.; Baiker, A.; Edwards, P. P. *Langmuir* **1993**, *9*, 2301.

(36) Supporting Information.

(37) Weiser, H. B. *The Colloidal Elements*; Wiley: New York, 1933.

(38) Duff, D. G.; Baiker, A.; Gameson, I.; Edwards, P. P. *Langmuir* **1993**, *9*, 2310.

(b) Hollow Gold Shells. Hydrofluoric acid (0.67 mL, 5 vol %) was added to 1 mL of a solution of gold shells (containing, e.g., 0.5 mg of particles with a 42 nm gold shell and a 205 nm radius silica core). After standing for 15 min, the solution was diluted with 18.33 mL of water. After sedimentation of the colloidal gold shells (without centrifugation), the supernatant was removed and the colloidal gold shells were redispersed in 20 mL of water and ultrasonicated for 10 min. This cleaning procedure was repeated at least two times.

(c) Silica-Covered Gold Shells. An outer silica shell around the gold shells was formed in two steps. The procedure is a modification of the method to cover small gold nanoparticles (15 nm diameter) with silica as described by Liz-Marzan et al.[12]

First a precursor shell was formed in aqueous solution. Aqueous sodium silicate solution (1.83 mL, containing 2.16×10^{-2} wt % SiO_2, pH ≈ 9.5) was added dropwise to 15 mL of a dilute aqueous solution of gold shells containing 6.9 mg of particles with a 31 nm gold shell and a 205 nm radius silica core (total gold surface ≈ 0.76 m^2/L; pH ≈ 5.5) under vigorous magnetic stirring (600 rpm). After the addition of the sodium silicate solution, the resulting dispersion (pH ≈ 8) was stirred (600 rpm) for 12 h.

To complete the formation of the sodium silicate precursor shell, 60 mL of ethanol was added under vigorous magnetic stirring (1000 rpm) to the reaction mixture and the dispersion was stirred for another 5 h. Because of the much lower solubility of sodium silicate in ethanol,[39] silica precipitates on the gold shells during this reaction step. To remove all still unreacted sodium silicate and small new silica nuclei eventually formed, the dispersion was centrifuged (100*g*) two times and redispersed in ethanol. Subsequently, the particles were redispersed in about 1.5 mL of ethanol, so that the particle concentration in the dispersion was about 4.7 g/L (6×10^{-2} vol %).

The thin silica precursor shells around the colloidal gold shells were grown further by a variation of the Stöber method.[12,33] An ammonia solution (10 vol % ammonia (29.3 wt % NH_3) in ethanol) was added under magnetic stirring to the reaction mixture followed by 53 μL of a TES solution (10 vol % in ethanol). The reaction mixture was stirred for another 12 h.

(iii) Characterization. Various methods to analyze composition, structure, and optical properties of the synthesized particles were used:

(a) TEM. Samples for transmission electron microscopy were prepared by dipping copper 400-mesh carrier grids covered with carbon-coated Formvar films in the dispersions ($c \approx 0.5-5$ g/L).

The attachment of the small gold nanoclusters to the silica spheres and the uniformity, completeness, and roughness of the gold shells formed and the silica-covered gold shells were studied with a Philips CM 200 FEG high-resolution transmission electron microscope (HRTEM) operated at 200 keV.

To determine particle radii and relative standard deviations of the particles synthesized in the different reaction steps, micrographs obtained on a Philips CM 10 transmission electron microscope operated at 80 keV were used. A diffraction grating was used to calibrate the magnification. At least 200 particles were analyzed per sample.

(b) SEM. Scanning electron microscopy (SEM) was also used to study the uniformity, completeness, and roughness of the colloidal gold shells. The same grids already prepared for the TEM studies were used. The measurements were carried out with a Philips XL30 FEG scanning electron microscope.

(c) Extinction Spectroscopy. The ultraviolet/visible extinction spectra of the colloidal gold shells and of the small gold clusters were measured from dilute aqueous solution in 1.00 cm quartz cells using a Cary 5 UV/visible/NIR spectrometer.

(d) Confocal Microscopy. To obtain confocal micrographs of the particles with a RITC labeled silica core and a gold shell, about 20 μL of a dilute aqueous dispersion ($c \approx 0.5$ g/L) was spread and dried on a microscope cover slip of 0.15 mm thickness and 22 mm diameter. The measurements were carried out in the reflection and the fluorescence mode simultaneously with a Leica inverted microscope (DM IRB) equipped with a Leica confocal scanning unit (TCS NT) and a combined krypton/argon mixed gas laser. We used a 100× oil immersion objective lens (Leica) with a numerical aperture of 1.4. The particles were excited at 568 nm, and the fluorescent light was detected above 590 nm.

To obtain a micrograph of a crystal of gold shells, a little glass vial (content: 1.7 mL) of which the bottom had been replaced by a microscope cover slip of 0.15 mm thickness was filled with 1.7 mL of a gold shell dispersion ($c \approx 2$ g/L). After 1 day, all particles were sedimented and had formed a crystal on the bottom. The confocal microscopy measurements were carried out in reflection mode ($\lambda = 633$ nm) with a Leica inverted microscope (DM IRB) equipped with a Leica confocal scanner (TCS SP2-x1) and a helium/neon laser. A 100× oil immersion objective lens with a numerical aperture of 1.4 (Leica) was used.

Results and Discussion

(i) Gold Shells with a Silica Core. (a) **Syntheses.** *Gold-Functionalized Silica Particles.* By the stepwise seeded Stöber growth process, spherical silica particles with a radius of 99 and 205 nm were grown. The polydispersity of the silica spheres decreased with every growth step, as reported before,[29] and was for the particles obtained 5.0% and 3.0%, respectively. Functionalization of these particles with APS and the centrifugation/redispersion steps did not influence their size and polydispersity as determined by TEM. The resulting particles were stable for at least 6 months and were used in all subsequent reaction steps.

The small gold nanoclusters were prepared by reduction of chloroauric acid with THPC exactly as described by Duff et al.[35,36] Because of the relatively short stability of the gold clusters, only fresh small gold nanoclusters produced less than 1 h before the addition to the amino-functionalized silica particles were used in the subsequent syntheses.[36]

The attachment of the small gold nanoclusters to the APS-treated silica spheres was carried out as described by Westcott et al.[32] For details see ref 36.

For the formation of the gold shell in the next reaction step, it is important that all nonattached small gold nanoclusters are removed from the dispersion of the gold-functionalized silica spheres. Several centrifugation/redispersion steps were necessary before extinction measurements indicated a negligible amount of gold clusters in the supernatant. It was found advantageous to wait 5 days before the growth of the shells, as it turned out that during this period the number of gold particles still in solution decreased significantly by Ostwald ripening,[40] while the seed colloids on the silica spheres were still smaller than 5 nm, as indicated by TEM and extinction measurements.[36]

Shell Growth. A method for the formation of gold shells by the reductive growth of small gold nanoclusters on silica spheres was already developed by Oldenburg et al.[14,17] Here the strong reduction agent sodium borohydride was used to reduce hydrogen tetrachloroaurate. This causes the further growth of most of the small gold particles attached to the spheres but, according to our findings, also results in a significant new nucleation of many new gold particles in the solution. We also found that these newly formed particles often start to coalesce into fractal-like clumps, which could not be removed from the gold shell particles.

The principal idea of the formation of a gold shell described here is to grow the small gold nanoclusters attached to the silica surface larger by more gentle reduction of gold onto them. After some initial growth these gold particles begin to coalesce, and finally a

(39) Buining, P. A.; Liz-Marzan, L. M.; Philipse, A. P. *J. Colloid Interface Sci.* **1996**, *179*, 318.

(40) Ostwald, W. *Lehrbuch der Allgemeinen Chemie*; Engelmann: Leipzig, 1896.

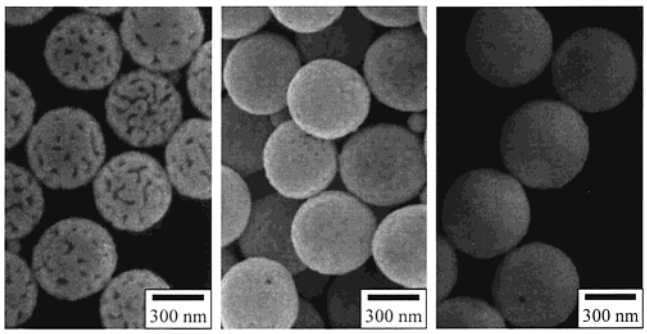

Figure 2. SEM pictures of silica particles (205 nm radius) with an incomplete gold shell of 23 nm (a), with a nearly complete gold shell of 39 nm (b), and with a thick gold shell of 63 nm (c).

continuous gold shell is formed. These shells may then be grown further to a thicker shell. To get well-defined, uniform, and closed shells, it is important that all small gold nanoclusters are growing simultaneously (e.g. not only the largest seeds) so that, after the clusters have grown a few nanometers, all clusters have coalesced and the resulting gold shell acquires a uniform thickness. This requires a relatively strong reduction agent for the gold salt. On the other hand, it is important that the newly added gold ions are only reduced on the small gold nanoclusters attached on the gold shells. Besides growth on gold clusters in the solution, the new nucleation of gold nuclei should also be prevented. This requires a reduction agent, which reduces gold salts only on already existing gold surfaces. First methods for the seeded growth of gold colloids were already developed by Zsigmondy.[41] Thiessen showed that, by using a reducing agent like hydroxylamine, gold nuclei already present could be grown further while the formation of new nuclei is suppressed.[42] This method was modified by Weiser[37] and used by Duff et al.[38] for seeded growth on clusters.

We have therefore combined the methods of Oldenburg et al. and Duff et al. and used hydroxylamine hydrochloride for the formation of the gold shells by the reductive growth of small gold seeds on silica spheres. As HRTEM measurements show, not all, but most of, the gold clusters distributed over the surface of the whole particles were growing at the same time by using this reducing agent. Thus, after an increase of the diameter of the gold clusters of about 20 nm, a shell of 23 nm thickness was reached (see Figure 2 a) although it was not yet a complete shell.

Further growth leads to the formation of uniform and more closed shells (shell thickness > 25−30 nm; see, e.g., Figure 2b and c). The polydispersity of the silica particles with a gold shell is only slightly higher than the polydispersity of the initial silica particles (see Table 2). If the silica particles functionalized with gold nanoclusters were prepared exactly as described above and especially the number of free gold nanoclusters was minimized before the addition of the $HAuCl_4/K_2CO_3$ and $NH_2OH{\cdot}HCl$ solutions, then nearly all added gold ions were used in the shell formation. This makes it possible to calculate the thickness of the obtained gold shells from the added amounts of gold salt and the size and concentration of the silica spheres used (see Table 2 and Experimental Section). The agreement with the measured data is good.

A small number of small gold clusters, which were not attached to the silica spheres but still existed in the dispersion and had also grown further by reduction of chloroauric acid, could be removed by (several) centrifugation/redispersion steps.

(41) Zsigmondy, R. *Z. Phys. Chem.* **1906**, *56*, 65.
(42) Thiessen, P. *Kolloid-Beih.* **1929**, *29*, 122.

Table 2. Size and Polydispersity of Gold Shells

			sphere radius			shell thickness	
sample	core radius (nm)	σ^a (%)	calc^b (nm)	meas^c (nm)	σ^a (%)	calc^b (nm)	meas^c (nm)
C1S1	99	5.0	122.1	128	5.7	22.9	29
C2S1	205	3.0	239.2	241	6.0	34.4	36
C2S2	205	3.0	251.3	247	5.1	46.4	42
C2S3	205	3.0	270.1	268	4.9	65.2	63
C2S4	205*/244**	3.0	292.8	287	4.9	87.9	82

[a] σ: relative standard deviation obtained by analysis of the TEM pictures (see Experimental Section). [b] calc: sphere radii and shell thickness which where used to calculate the amounts of the chemicals used in the shell formation reaction (see Experimental Section). [c] meas: sphere radii obtained by TEM measurements (see Experimental Section); shell thickness obtained by subtraction of the core radii (also obtained by TEM measurements) from this value.

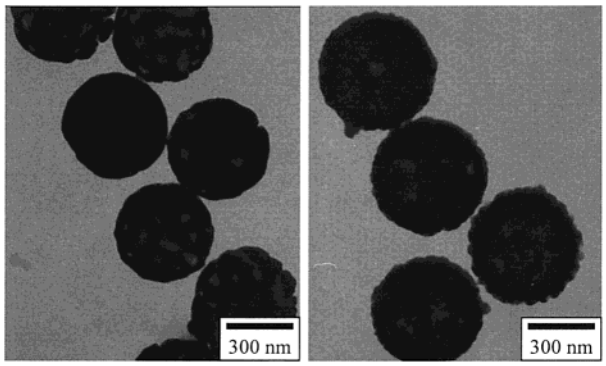

Figure 3. Formation of a thick gold shell by reduction of hydrogen tetrachloroaurate on silica particles with a thinner gold shell. TEM pictures of silica particles (205 nm radius) with a 39 nm incomplete gold shell (a) and silica particles with a 82 nm nearly complete gold shell obtained by a second $HAuCl_4$ reduction on these spheres (b).

All shell growth reactions were carried out at low $HAuCl_4$ (0.435 mM) and $NH_2OH{\cdot}HCl$ (1.875 mM) concentrations, as in the method described for the growth of small gold nanoclusters by Duff et al.[38] Consequently, the concentrations of the gold-covered precursor silica particles also had to be low (typically 10^{-3} to 10^{-4} vol %). At higher concentrations the dispersions were found to aggregate. Lower $K_2CO_3/HAuCl_4$ ratios led to similar results. Work is going on to increase the volume fraction of the precursor particles in the gold shell particle synthesis.

If a thick gold shell has to be grown in one step, it becomes difficult to remove the small amount of gold particles growing freely in solution. Therefore, we used a two-step process to produce particles with a gold shell of 88 nm: First, silica spheres with a thin gold shell were synthesized (see Figure 3 a). Then these particles were cleaned up and the gold shell was grown by the same procedure as described before to the desired final thickness (see Figure 3b and Table 2). Also in this case, the polydispersity was as low (<5%) as that for spheres with thinner gold shells formed in one step (see Table 2). However, the surface of these particles was less smooth. It is likely that a similar procedure can also be used to grow a different metal shell, for example, silver, on top of the gold shells.

The gold shell particles obtained by the method described in the last few paragraphs are stable in water or

ethanol for several weeks to months. After a longer period, aggregates formed which could only partially be broken up by ultrasonication.

(b) Optical Properties. Optical extinction[43] spectra of gold shell particles with different core and shell sizes were measured in water. To compare these spectra with theory, a program for the calculation of optical spectra of particles with multiple shells based on Mie theory[4,31] was used. The calculations require as input the refractive indices of the silica core (1.43, assumed to be constant compared to the high dispersion of gold) and the embedding medium ($n = 1.33$), the frequency-dependent dielectric constant of gold,[44] the size of the core, and the thickness of the shell. The polydispersities of the core and the shell were also taken into account.

Extinction spectra were initially calculated with the data for the silica core radii obtained by TEM measurements, and the thickness of the gold shells was calculated by subtraction of these core radii from the total particle radii also obtained by TEM. These spectra were then adjusted to the measured extinction spectra by a fitting procedure. For a given shell thickness, the positions of the peaks due to dipole, quadrupole, and higher order resonances in the extinction spectrum are strongly dependent on the size of the core. Small variations in the thickness of the gold shell have, for a constant core size, a less important influence on the positions of the plasmon resonances but do influence the general shape of the extinction curve. These different influences of core and shell size on the extinction spectrum make it possible, for the sizes we studied, to obtain both the core radius and the gold shell thickness by fitting of the extinction spectra. The polydispersity of the silica cores causes mainly a "line broadening" but not a shift of the resonance modes. From the TEM measurements (see Table 2) it is clear that the polydispersity in the thickness of the shells cannot be larger than 20%. Such a polydispersity hardly changes the features of the spectra and therefore was not taken into account.

The measured and calculated spectra of the particles with a (nearly) complete gold shell correspond well (see Figures 4 and 5). Small deviations may be due to the presence of a small number of particles with an incomplete gold shell and small gold particles without silica cores (see Syntheses). Particles with an incomplete gold shell (see Figure 2a and solid line in the inset in Figure 4) show a completely different spectrum than those with a closed or nearly closed gold shell (see dotted line in Figure 4).

The spectrum of the silica particles with a nearly closed gold shell shown in Figure 4 is shifted about 20 nm to longer wavelength compared to that of particles with a thicker shell and a core of equal size (217 nm; Figure 5a), in accordance with theory. A comparison of these two spectra with the spectrum of gold particles with a significantly smaller core (114 nm) demonstrates the important influence of the core size on the optical properties of the gold shell particles: While for the particles with a small core the extinction spectrum is mainly determined by dipole and quadrupole contributions and shows only a single strong peak at 680 nm which corresponds to the maximum of the quadrupole resonance, the spectra of the particles with a bigger core (Figures 4 and 5a) have additional contributions of octupole and higher order resonances and are therefore more complicated functions with several maxima.

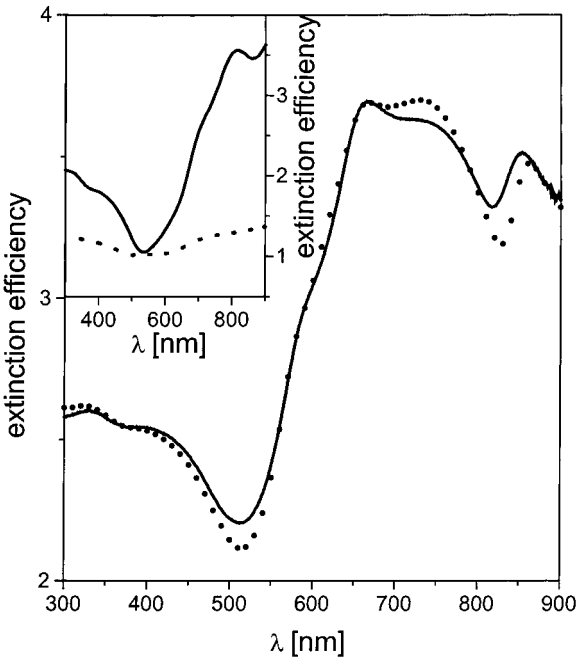

Figure 4. Extinction spectrum of gold shells with a silica core of 205 nm radius (TEM data) and a nearly complete gold shell of 39 nm (TEM data, solid line). The dotted line is a calculated spectrum for these particles considering that because of shrinkage during the TEM measurements the real radii of the pure silica particles are 6% larger and those of the gold-covered particles are about 2% larger. Because of the different degrees of shrinkage of covered particle and core, the corrected gold shell thickness is 32 nm. The core polydispersity in the calculated spectrum is 1% (measured 3%). Inset: Extinction spectrum of particles with a silica core of the same size and an incomplete shell of 23 nm (TEM data, solid line). For the calculation of the theoretical spectrum (dotted line) of particles with the same composition but a closed shell, a corrected core radius of 217 nm, a gold shell thickness of 15 nm, and a core polydispersity of 1% were assumed.

In Figure 5 the contributions of the absorption (open triangles) and scattering (filled squares) are shown separately for the fitted data. Because of the approximately doubled radius of the core, the relative contribution of the scattering to the total optical extinction for the gold shell spheres shown in Figure 5 a is significantly higher than that for those shown in Figure 5b.

For all the samples with a silica core of the same size (205 nm radius, TEM data) and varying shell thickness, always about 6% larger core radii were obtained from extinction spectra. For silica particles it has often been observed that the radii obtained by TEM measurements are smaller than the radii obtained by dynamic light scattering in solution. This is ascribed to shrinkage of the spheres caused by electron beam damage and the vacuum in the TEM microscope.[45,46] For the particles with a gold shell it is difficult to obtain radii by dynamic light scattering because of absorption, so that the degree of shrinkage during TEM measurements is unknown. However, the fitted values for the thickness of the gold shell were significantly smaller than those obtained by the subtraction of the core from the total sphere radii obtained from the TEM measurements. Apparently, the size of the gold-covered particles determined by TEM was less

(43) Extinction efficiency = (scattering cross section + absorption cross section)/(geometrical cross section).[31]

(44) Palik, E. D. *Handbook of Optical Constants of Solids*; Academic Press: New York, 1985.

(45) van Helden, A. K.; Jansen, J. W.; Vrij, A. *J. Colloid Interface Sci.* **1981**, *81*, 354.

(46) van Blaaderen, A.; Kentgens, A. P. M. *J. Non-Cryst. Solids* **1992**, *149*, 161.

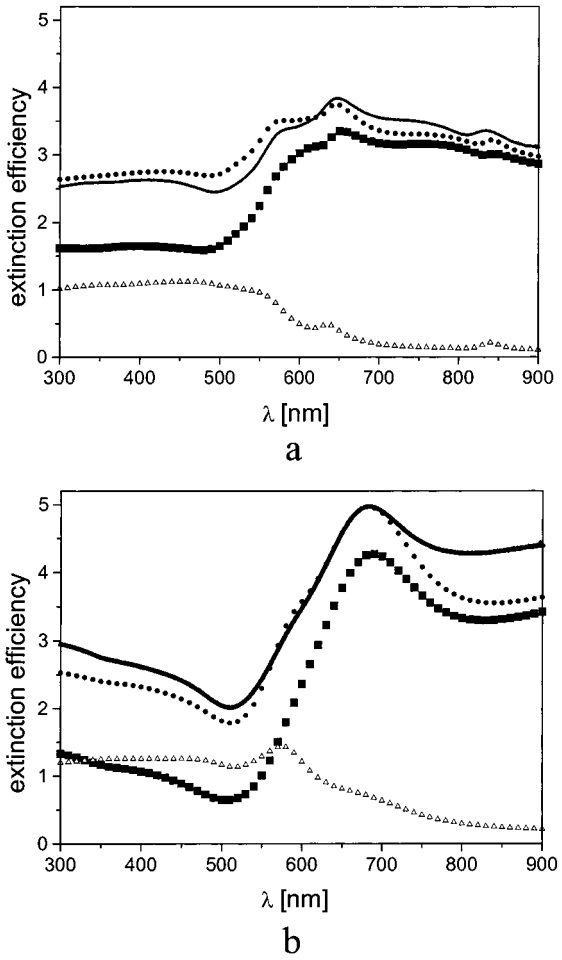

Figure 5. Measured (solid line) and calculated (solid circles) extinction spectra shown together with the contributions from absorption (open triangles) and scattering (solid squares) of gold shells with a silica core. (a) Silica particles (205 nm radius) with a complete gold shell of 63 nm (TEM data). From the fit it was found that because of shrinkage during the TEM measurements the real radii of the pure silica particles are 6% larger, while the gold-covered particles do not shrink during these measurements. The corrected gold shell thickness is 51 nm. The core polydispersity in the calculated spectra is 1% (measured by TEM: 3%). (b) Silica particles (99 nm radius) with a nearly complete gold shell of 29 nm (TEM data). From the fit it was found that because of shrinkage during the TEM measurements the real radii of the pure silica particles are 15% larger and those of the gold-covered particles are about 7% larger. The corrected gold shell thickness is 23 nm. The core polydispersity in the calculated spectra is 2% (measured by TEM: 5%).

influenced by electron beam damage than that of the pure silica particles, leading to an overestimation of the shell thickness by simple subtraction. However, it is not clear if the silica underneath the shell still shrinks and/or that the gold prevents the shrinkage from happening. Moreover, it turned out that the more complete the gold shells are, the less the radius as determined from the extinction spectrum deviated from the electron microscopy measurement. While for particles with only nearly complete gold shells the summation of the fitted core size and shell thickness indicates that these particles still shrink about 2% during the TEM measurements (see Figure 4 and Figure 5b), particles with a thick and complete gold shell do not shrink due to electron beam damage in the TEM microscope (see Figure 5a). The shrinkage we find was not reported before,[14,17] perhaps because our samples are more monodisperse.

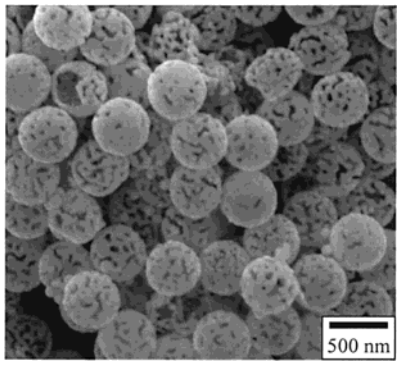

Figure 6. SEM pictures of hollow gold shells with an incomplete shell of 23 nm. The dissolved core had a radius of 205 nm (for particles before HF treatment: see Figure 2a).

For particles with a smaller silica core (99 nm radius, TEM data), we found a more severe shrinkage during the TEM measurements of the particles of about 15% (Figure 5b). This is in accordance with results in ref 46, where it has been shown that the shrinkage of silica spheres caused by electron beam damage and the vacuum in the TEM microscope is more important for smaller particles because of their lower density.

Surprisingly, the polydispersity of the silica cores was, according to the comparison of measured and calculated spectra, significantly smaller than the results from the analysis of the TEM micrographs: only 1% for the particles with the bigger silica core (TEM: 3%) and about 2% (TEM: 5%) for those with a smaller core.

The comparison of the measured extinction spectra with theoretical calculation shows a good agreement of the data obtained with theory and demonstrates the possibilities to adjust the optical properties of the gold-covered silica spheres with the synthesis method described here. Because the extinction data are taken in solution, they give a better representation of the "true" particle size.

(ii) Hollow Gold Shells. By treatment with dilute hydrofluoric acid, the silica core of the gold shell particles could be dissolved:

$$SiO_2 + 4HF \rightarrow SiF_4 + 2H_2O \qquad (1)$$

In this way, hollow gold shells can be obtained if the gold shell is still permeable to the acid and the dissolved silica. For the particles with a not completely closed shell, this was easily shown by TEM or SEM measurements. Figure 6 shows a typical example of such porous empty gold shells (core radius, 205 nm; shell, 23 nm) after HF-treatment; in Figure 2a particles of the same sample are shown before the dissolution of the core.

If the gold shell is almost completely closed, it is more difficult to judge if the silica cores are dissolved or not, because for those particles there is nearly no visible change in the electron microscopy pictures. According to calculations, removing the core should also lead to a significant shift of the maximum of the extinction spectrum to shorter wavelengths (see inset in Figure 7), which is caused by a change of the refractive index of the "core" from 1.45 (silica) to 1.33 (water). The relatively good agreement between the measured and the calculated spectra, for which a closed shell is assumed, shows that the majority of the cores of particles with a thicker and nearly complete shell (42 nm) were dissolved with hydrofluoric acid (Figure 7). This also demonstrates that the dissolution of the silica core allows a further adjustment of the optical properties of the gold shell particles.

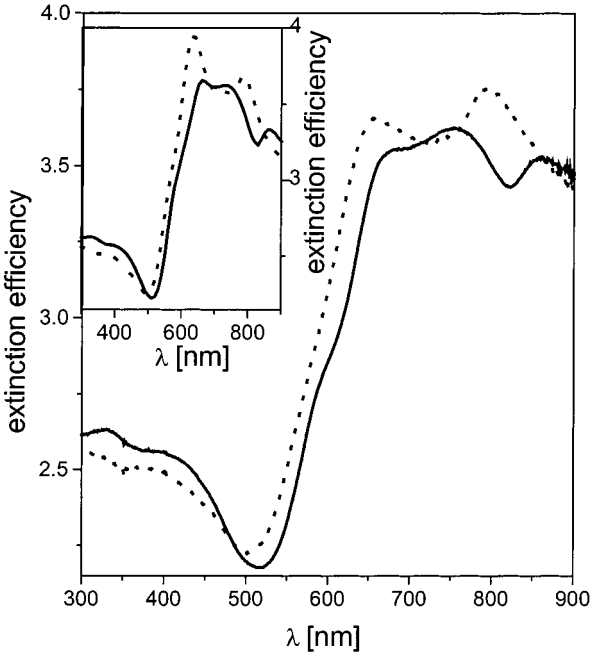

Figure 7. Extinction spectra of gold shells with a nearly complete shell of 42 nm (TEM data) before (solid line) and after (dotted line) the dissolution of the core (205 nm radius, TEM data) measured in water. Inset: Calculated extinction spectra with (solid line) and without (dotted line) silica core, considering that because of shrinkage during the TEM measurements the real radii of the pure silica particles are 6% larger and those of the gold-covered particles are about 2% larger. The corrected gold shell thickness is 35 nm. The core polydispersity in the calculated spectra is 2% (measured by TEM: 3%).

To show more distinctly that it is possible to produce empty gold shells by the method described here and also to test the permeability of gold shells that seemed closed in electron microscopy, we investigated particles with a fluorescent silica core and a gold shell. Silica particles with a core (92 nm radius) containing tetraethylrhodamineisothiocyanate (RITC) groups and a shell of pure silica (96 nm)[20] were covered with a gold shell. The thickness of the gold shells measured by TEM was about 22 nm. Compared to the cases of samples shown and discussed above, the polydispersity of these dye-labeled silica cores was slightly higher (8.1%). Also, the variance in the thickness and completeness of the gold shell of this sample was slightly higher, which was probably caused by the polydispersity of the precursors. Note that this sample contains many ($^1/_3$) particles with an incomplete, porous shell and also a lot of particles with a thick closed shell (Figure 8a).

Confocal microscopy images were taken simultaneously in fluorescence and reflection mode. In reflection mode all particles of the sample are visible due to the strong scattering of the gold shells. Tetraethylrhodamineisothiocyanate (RITC) labeled silica particles without a gold shell show strong fluorescence when they are excited with light at or close to the absorption maximum of RITC (555−580 nm).[20] In Figure 8b (reflection mode) and c (fluorescence mode) the particles before the treatment with HF are shown. The rhodamine cores were excited with light of 568 nm wavelength, and the fluorescence at wavelengths ≥ 590 nm was detected (see Figure 8c). The pictures in reflection and in fluorescence modes are practically identical; apparently, the filtering effect of the gold shells on excitation and detection of the rhodamine fluorescence is not too strong. After the reaction with HF (see TEM picture Figure 8d), only about 5% of the particles still fluoresced if excited with light of 568 nm wavelength, while in the reflection mode all gold shells were still visible (see Figure 8e and f). The confocal microscopy pictures were taken in exactly the same way as the pictures in Figure 8b and c of the untreated sample. It can be concluded, therefore, that the silica cores of about 95% of these gold shell particles were completely dissolved by the reaction with hydrofluoric acid. As the comparison with TEM measurements (Figure 8d) indicates, many particles with a nearly complete gold shell are empty after this reaction step. As long as the gold shell has some small holes, the inorganic core can be completely dissolved. As shown above (Figure 7), these particles with a nearly complete but still permeable gold shell already show extinction spectra very similar to the theoretical spectra of perfectly closed gold shell particles (see inset in Figure 7). On the other hand the obtained results demonstrate that a gold shell that is impermeable to HF and/or the dissolved silica can be made by this method as well.

The hollow gold shells aggregate more easily than the particles with a silica core, probably because after the dissolution of the silica core the charge density is reduced. Usually, after some hours nearly the complete sample is aggregated. These aggregates can be to a large extent redispersed by short ultrasonification of the dispersions.

(iii) Silica-Covered Gold Shells. A method to cover small citrate-stabilized gold particles (15 nm diameter) homogeneously with silica was developed by Liz-Marzan et al.[12] In that work, the gold particles are first surface-functionalized with APS in water. Then, a silica shell of variable thickness is created by first applying a coating of a thin shell from water−glass in aqueous solution and a further seeded Stöber growth in ethanol. We obtained a smooth silica shell without the APS coating and by modifying the water−glass coating procedure.

We arrived at this procedure after making the following observations: By carrying out the silica coverage reaction in exactly the same way as described in ref 12 for creation of a 50 nm thick silica layer, only irregular and incomplete silica shells on only parts of the gold shells were obtained. Nevertheless, the stability of the particles was not influenced by the coating procedure. Neither by a further addition of TES nor by varying the amount of APS for the primary surface functionalization could these results be improved. Moreover, it turned out that without addition of APS the same results were obtained.

In addition, we found that, contrary to the small citrate-stabilized gold particles used in ref 12 which are only stable in water but not in ethanol unless they have a silica shell formed from sodium silicate of a sufficient thickness of about 2−4 nm,[12,47] the gold shell particles are in any stage of the reaction stable in water and ethanol. This made it possible to transfer the particles directly after the addition of APS to ethanol to perform a seeded Stöber growth without first depositing a precursor silica shell from water−glass. But also in this case, the same results were obtained as before: Only a few particles were covered with incomplete silica shells, while the stability of the particles was not influenced. Apparently, the precursor shells are necessary for the formation of a homogeneous silica coating like in ref 12 in the subsequent Stöber growth step but were not thick enough when we tried to reproduce the procedure of ref 12 in our case.

The polymerization/precipitation of sodium silicate in water is a relative slow and not very well controlled process; for example, the time needed to grow a sodium silicate shell of about 2−4 nm around the small citrate-

(47) Graf, C.; van Blaaderen, A. In preparation.

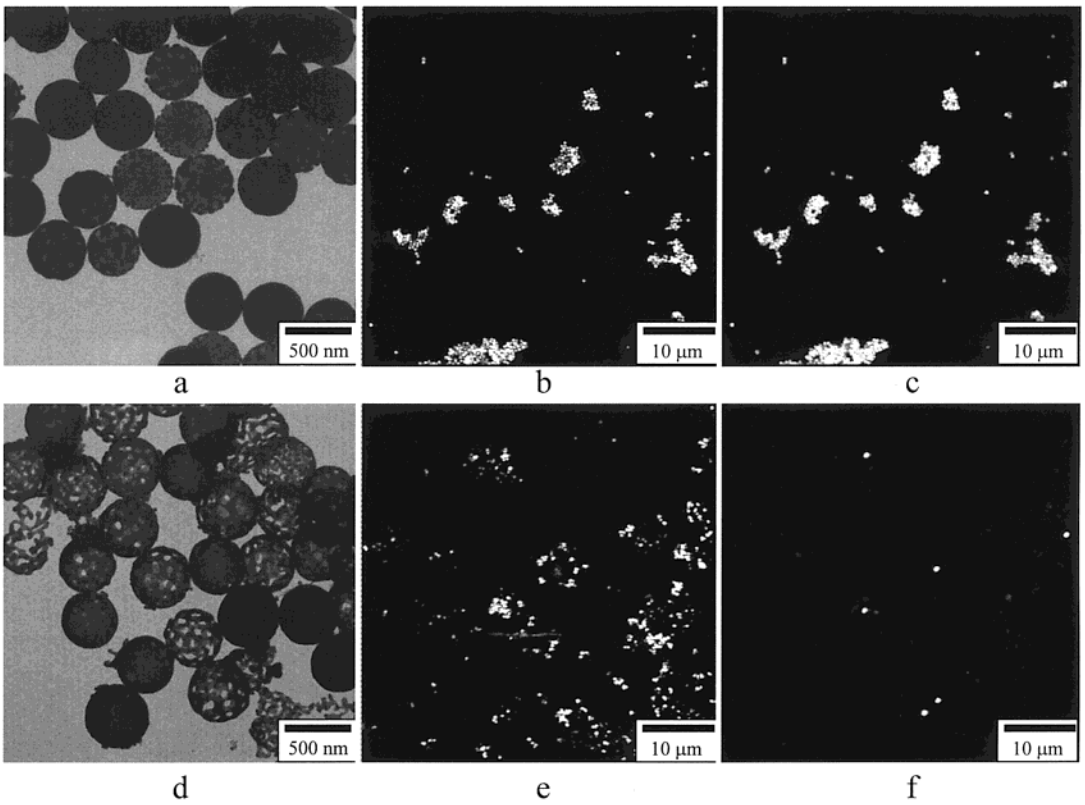

Figure 8. Confocal microscopy measurements of silica spheres (188 nm radius) with a rhodamine-labeled core (92 nm radius) and a gold shell of 22 nm. (b) Reflection ($\lambda = 568$ nm) and (c) fluorescence picture ($\lambda_{EX} = 568$ nm) before and (e) reflection ($\lambda = 568$ nm) and (f) fluorescence picture ($\lambda_{EX} = 568$ nm) after the dissolution of the core. For comparison: TEM pictures of the same sample before (a) and after the dissolution of the core (d).

stabilized gold particles may vary between 24 h and 8 weeks under practically identical conditions (sodium silicate concentration, about 2×10^{-2} wt % SiO_2[12,47]). The procedure we finally arrived at to quickly and reproducibly get a thick enough precursor shell from water−glass was based on a procedure of Buining et al.,[39] namely a sudden lowering of the silicate solubility by the addition of ethanol. For instance, particle formation takes place instantaneously when a relatively dilute aqueous solution of sodium silicate (0.22 wt % SiO_2) is added to ethanol (final sodium silicate concentration, 5.3×10^{-3} wt % SiO_2).[39] In the case of the small gold particles, the direct addition of an excess of ethanol to the aqueous solution (ethanol/water ratio, 4:1; final sodium silicate concentration, 4.1×10^{-3} wt % SiO_2) leads to partial aggregation of the system. However, in the case of the gold shell particles, the addition of an excess of ethanol (ethanol/water ratio, 4:1; final sodium silicate concentration, 4.7×10^{-4} wt % SiO_2) did not influence the stability of the system but led to the formation of a sufficiently thick silica precursor shell. Probably this is due to the 1 order of magnitude lower sodium silicate concentration.

Before the subsequent Stöber growth step, it was important to reduce the volume of the solution because the smaller the total surface area the more new particles were formed during such a growth process.[48] According to Chen et al.,[48] to prevent second nucleation for the used particles of 236 nm radius, the total surface area should be at least about 5 m^2/L.

In this way, gold shell particles could be reproducibly covered with a homogeneous and smooth silica shell (see Figure 9).

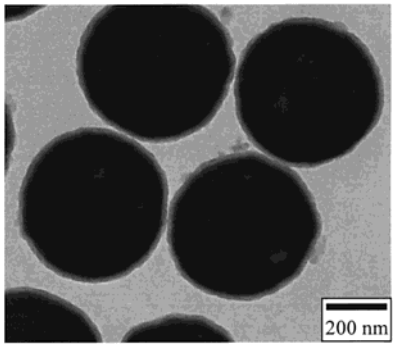

Figure 9. TEM picture of silica particles (205 nm radius) with a 31 nm gold shell and an outer silica shell of 20 nm.

In conclusion, it is important for a complete and homogeneous coverage of the gold shells that the silica shell formation is started by the polymerization/precipitation of the oligomeric silicate species contained in the sodium silicate solution on the gold surface before a homogeneous shell from tetraethoxysilane monomers can be formed. In contrast to the results obtained for the small citrate-stabilized gold particles,[12] a previous functionalization of the gold surface with a silane-coupling agent is not required. This may be caused by the different stabilization of the gold shell particles. Direct coating of silica without the use of a silane coupling agent was recently also reported for surfactant-stabilized silver particles.[49]

(iv) Crystallization. The gold shell particles sediment fast because of their relatively high density (about 8−10

(48) Chen, S.-H.; Dong, P.; Yang, G.-H.; Yang, J.-J. *J. Colloid Interface Sci.* **1996**, *180*, 237.

(49) Hardikar, V. V.; Matijevic, E. *J. Colloid Interface Sci.* **2000**, *221*, 133.

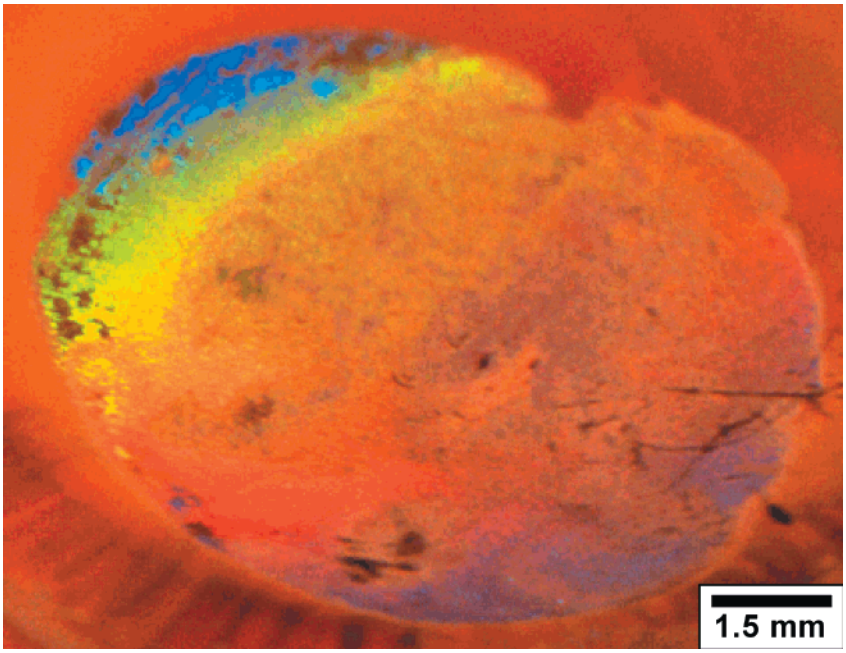

Figure 10. Photograph of a crystal formed of silica particles (205 nm radius) with a 31 nm gold shell sedimented in water.

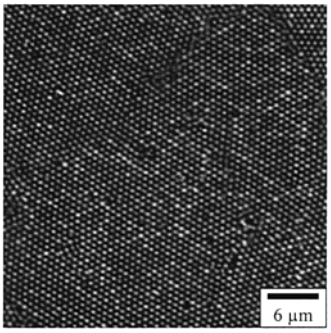

Figure 11. Confocal microscopy picture (reflection mode $\lambda =$ 633 nm) of silica particles (205 nm radius) with a 36 nm gold shell sedimented in water (interparticle spacing about 320 nm).

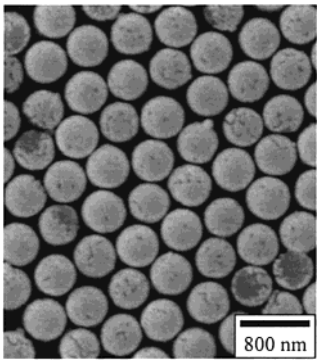

Figure 12. SEM picture of silica particles (205 nm radius) with a 48 nm gold shell and an outer silica shell of 10 nm dried from ethanolic solution on a silicon waver.

g/cm^3, depending on the core/shell ratio). Despite their fast sedimentation, the particles do crystallize in the sediment due to their low polydispersity of about 5% (see Table 2) and their high surface charges. Figure 10 is a photograph of a typical crystal formed of silica particles (205 nm radius) with a 31 nm gold shell after sedimentation in water for 12 h.

Because of the long-range order of the system and the submicron lattice parameter, this crystal shows colorful Bragg reflections.

To obtain a measurement of the interparticle spacing and the defects and the symmetry of the crystals formed from the gold shells, several samples were investigated by confocal microscopy. Figure 11 shows the bottom layer of a crystal of silica particles (205 nm radius) with a 36 nm gold shell sedimented in water.

The picture was taken in reflection mode. The center-to-center distance of neighboring particles is about 800 nm, significantly larger than the particle diameter (482 nm), because of the surface charge of the particles and the low concentration of salt. The extended range of the interaction by the double-layer overlap decreased the effective polydispersity even further.

Dried crystals of gold shell particles (from aqueous or ethanolic solutions) could not be obtained. Because of strong van der Waals interparticle forces and interaction with, for example, the glass surface, the particles aggregate during the drying process before they can form an ordered structure. From silica particles made by seeded Stöber growth, dried crystals could easily be obtained,[50,51] so that the additional silica coverage of the gold shell particles described in the previous section facilitates the formation of colloidal crystals with a high volume fraction. Figure 12 shows a sample of silica-covered gold shell particles dried from ethanol on a silicon waver. Because of the 10 nm thick silica shell, the strong interactions between the particles and with the surface were so far reduced that interparticle aggregation could be prevented and the particles formed a hexagonal ordered close-packed structure. Work to obtain larger crystals of such silica-covered gold shell particles is in progress.

Conclusions

We have modified an existing procedure for the formation of gold shell particles with a dielectric core.[14,17] By using hydroxylamine for the reduction of $HAuCl_4$ onto small gold nanoclusters attached to silica spheres, particles

(50) Denkov, N. D.; Velev, O. D.; Kralchevsky, P. A.; Ivanov, I. B.; Yoshimura, H.; Nagayama, K. *Langmuir* **1992**, *8*, 3183.
(51) Denkov, N. D.; Velev, O. D.; Kralchevsky, P. A.; Ivanov, I. B.; Yoshimura, H.; Nagayama, K. *Nature* **1993**, *361*, 26.

with a variable core radius, a well controlled gold shell thickness of about 20−80 nm, and a low polydispersity were obtained. The measured extinction spectra show good agreement with theoretical calculations and also demonstrate the possibilities to adjust the optical properties of the gold-covered silica spheres with this synthesis method. Further, we have shown that as long as the gold shell has a slight porosity it is possible to completely dissolve the silica cores of these particles. The creation of empty, almost complete gold shells leads to a larger surface area of the gold exposed and the possibility to fill the metal shells. Additionally, the dissolution of the core can also be applied after colloidal crystallization. We have also developed a reproducible method to cover these particles with a homogeneous silica layer. In contrast to methods reported for the coverage of small solid gold particles with silica,[12] a previous functionalization of the gold surface is not required. Subsequent seeded Stöber growth[27−29,48] and/or functionalization of these silica shells on the gold shells can increase the possible use of the metallodielectric spheres significantly. Because of their low polydispersity and their size, the gold shell silica core particles form colloidal crystals with lattice constants on the order of visible wavelengths.

Because of their monodispersity, their tunable optical properties, and their functionable silica shell, these particles may be used as building blocks for various applications such as for nanosecond optical switches[52] or metallodielectric photonic crystals[21−23] or as model particles to study the enhancement of nonlinear optical properties of dyes close to the metal colloid surfaces.[9]

Acknowledgment. The authors wish to thank Carlos M. van Kats for the SEM and parts of the HRTEM measurements and Alexander Moroz for the program for the calculation of the extinction spectra and, together with Krassimir P. Velikov, for helpful discussions. Arnout Imhof is acknowledged for the critical reading of the manuscript. Further, we thank Jan den Boesterd for the photograph of the crystal. This work was financially supported by the Foundation for the Fundamental Research of Matter (FOM), which is part of The Netherlands Organization for Scientific Research (NWO).

Supporting Information Available: Details on the synthesis and the characterization of the small gold nanoclusters and the attachment of the small gold nanoclusters to the APS-treated silica spheres. In addition, extinction spectra of the small gold nanoclusters, of silica spheres with attached small gold nanoclusters on the surface, and of the supernatant remaining after the first centrifugation step of such gold-functionalized silica spheres in water as well as the HRTEM picture of silica spheres with attached small gold nanoclusters are discussed. Finally, we give additional proof of the shrinkage of the particles caused by TEM measurements. This material is available free of charge via the Internet at http://pubs.acs.org.

LA011093G

(52) Pan, G. S.; Kesavamoorthy, R.; Asher, S. A. *Phys. Rev. Lett.* **1997**, *78*, 3860.